*Nanoporous Materials*

# Nanoporous Polyelectrolyte Spheres Prepared by Sequentially Coating Sacrificial Mesoporous Silica Spheres**

*Yajun Wang, Aimin Yu, and Frank Caruso**

Mesoporous silicas (MS), porous materials with extremely high surface areas and pore sizes in the range of 2 to 50 nm, have attracted significant interest since being reported in the early 1990s.[1,2] Owing to their unique pore structures, these materials have been utilized as hosts for the template synthesis of various materials, including metal,[3] metal oxide,[4] carbon,[5] and polymer[6] replicas. In a typical synthesis strategy, the constituent materials (e.g., metal precursors, sucrose, organic monomers) are infiltrated into the mesopores. Reduction, carbonization, or cross-linking reactions are then performed to obtain an interconnected network, and the silica template is removed by dissolution. Despite these studies, there has been no report on the sequential infiltration and coating of MS materials with preformed polymers for the fabrication of controlled porous polymer structures. Porous polymer materials, especially in particulate form, are of interest in a diverse range of applications, including drug delivery, molecular separation technology, and as hosts for chemical synthesis.[7]

A facile approach for coating MS is to exploit electrostatic interactions between the MS support and charged polymers (polyelectrolytes, PEs) through solution self-assembly. Sequentially depositing PEs of opposite charge by the layer-by-layer (LbL) technique would potentially permit the formation of PE multilayers inside the MS pores. Since its introduction in 1991,[8,9] the LbL method has been widely used to deposit multilayers of various materials (such as, polymers, enzymes, nanoparticles, dyes) on both planar[10] and colloidal[11] supports. More recent studies have focused on the use of porous substrates, such as macroporous titania,[12] polycarbonate membranes,[13] alumina membranes,[14] and porous calcium carbonate microparticles.[15] However, there has been no report of the LbL assembly of PEs in MS structures and, more specifically, of the LbL MS-templated formation of porous materials with interconnected polymer networks.

[*] Dr. Y. Wang, Dr. A. Yu, Prof. F. Caruso
Centre for Nanoscience and Nanotechnology
Department of Chemical and Biomolecular Engineering
The University of Melbourne
Victoria, 3010 (Australia)
Fax: (+61) 3-8344-4153
E-mail: fcaruso@unimelb.edu.au

[**] This work was supported by the Australian Research Council (Discovery Project and Federation Fellowship Schemes) and the Victorian State Government, Department of Innovation, Industry and Regional Development, Science, Technology and Innovation initiative. The Particulate Fluids Processing Centre is acknowledged for support. J. Quinn, Q. Li and B. Radt are thanked for assistance with SEM, FTIR, and CLSM experiments, respectively.

Herein, we report the LbL coating of MS spheres with PEs and the subsequent removal of the silica templates to obtain micrometer-sized nanoporous PE spheres (NPS). The procedure for the preparation of the NPS involves two main steps, as depicted in Scheme 1. The first entails the LbL deposition of oppositely charged PEs (poly(acrylic acid) (PAA) and poly(allylamine hydrochloride) (PAH)) within the MS spheres, with subsequent cross-linking of each PE layer by heating. In the second step, the MS template is removed by exposure to hydrofluoric acid (HF). A main advantage of this approach is that it offers a general and versatile route to the preparation of nanoporous PE materials of diverse and tailored composition, as it is based on sequential self-assembly. Hence, it is applicable to a broad range of PEs. Further, the LbL method is largely independent of substrate morphology, making it amenable to MS of different shapes and sizes to generate porous PE networks. Herein we focus on the use of spherical MS particles in the micrometer size range, as these systems represent an interesting class of materials as supports for immobilization and encapsulation of various species (e.g., biomacromolecules). In this study, we also demonstrate the high capacity of the prepared NPS for enzyme entrapment.

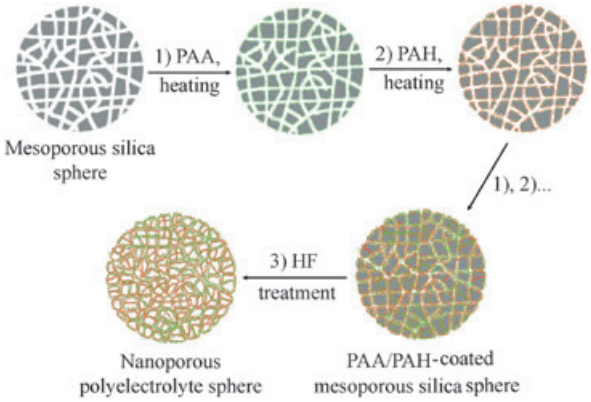


***Scheme 1.*** Schematic illustration showing the preparation of nanoporous polyelectrolyte spheres (NPS). 3-aminopropyltriethoxysilane (APTS)-modified bimodal MS (BMS) spheres were layer-by-layer coated with PEs of opposite charge (PAA and PAH; multiple repetition of steps 1 and 2), with the samples heated (160 °C for 2 h) after deposition of each PE to partially cross-link the layers. The BMS template was then dissolved by exposure to HF (step 3), yielding intact NPS.

The MS spheres, prepared according to an established method,[16] possess a bimodal pore structure; that is, smaller pores in the 2–3 nm range and larger pores between 10–40 nm.[16] The particles, herein denoted as BMS (bimodal MS) spheres, have a diameter of 2–4 μm, a surface area of 630 $m^2 g^{-1}$ and a pore volume of 1.72 $mL g^{-1}$. We chose to employ BMS spheres for several reasons: 1) BMS possesses a high pore volume (1.2 $mL g^{-1}$) for the 10–40 nm pores, making it suitable for infiltration and adsorption of PEs; 2) the three-dimensional disordered pore structure and thin pore walls (ca. 3 nm) facilitates the formation of interconnected nanoporous PE networks after removal of the BMS templates; and 3) the spherical morphology aids in monitoring shape and size

  DOI: 10.1002/ange.200462135 

variations as a result of LbL PE coating. The BMS surface was first functionalized by grafting a layer of 3-aminopropyltriethoxysilane (APTS) onto the BMS skeleton.[17] This process introduces amine ($NH_2$-) surface functional groups to the BMS, which promotes specific adsorption of the subsequently deposited PAA through interaction of the $-NH_2$ and $-COOH$ groups. The APTS-grafted BMS (APTS–BMS) spheres have a surface area of 465 $m^2 g^{-1}$ and a pore volume of 1.32 $mL g^{-1}$. The large mesopores (10–40 nm) have a volume of approximately 1.0 $mL g^{-1}$.

Polyelectrolyte solutions were prepared by dissolving PAA or PAH in deionized water containing sodium chloride (NaCl), without adjusting the pH value. PAA ($M_w = 2000$) was deposited onto the APTS–BMS spheres from an aqueous 5 $mg mL^{-1}$ PAA solution of pH 2.9 containing 0.7 M NaCl. Adsorption was conducted at 20 °C for 15 min with sonication (to aid the transport of the PEs into the mesopores[13]), and subsequent shaking for 6 h. Excess PAA was removed by four cycles of centrifugation (500 *g* for 3 min) and washing with 0.1 M NaCl. PAH ($M_w = 15000$) was deposited from an aqueous 5 $mg mL^{-1}$ PAH solution of pH 4.3 with 0.7 M NaCl. To facilitate infiltration into the pores of the APTS–BMS spheres, low molecular weight PEs were used,[13] and NaCl was added to the adsorption solution to promote coiling of the PE molecules.[18] Cross-linking of each PE layer was performed by heating the dried sample at 160 °C for 2 h.[19,20] Under this treatment, amide bonds are formed by the $-COOH$ groups (in PAA) and the $-NH_2$ moieties (in PAH or on the APTS–BMS template), enhancing the structural stability of the layers.[19,20] It was found that without the cross-linking process, the PE layers partially desorbed from the mesopores during subsequent PE adsorption steps, forming aggregates on the particle surface and in solution.[21]

Evidence for the successive deposition of PAA and PAH within the pores of the APTS–BMS spheres was obtained by Fourier transform infrared (FTIR) experiments. FTIR spectra of the APTS–BMS particles as a function of PAA and PAH deposition steps are shown in Figure 1 a. For the APTS–BMS spheres, the absorption band at 1635 $cm^{-1}$ (A) is assigned to the Si–OH vibrations[22] and the N–H bending (scissoring) vibrations of APTS. The peaks at 1720 (B), 1570 (C), and 1400 (D) $cm^{-1}$ are attributed to the $-COOH$ carbonyl and $-COO^-$ asymmetric and symmetric stretches, respectively, of PAA.[19,23] The large fraction of non-ionized acid groups in the PAA chains is caused by the low assembly pH value in our experiments.[24] The intensities of the peaks at 1635 $cm^{-1}$ (assigned to the N–H bending (scissoring) vibration of PAH for layer number = 2) and at 1720 $cm^{-1}$ increase with PAH and PAA layer number, respectively, confirming the sequential deposition of PAA/PAH multilayers. The following observations can be made from the spectra: a) The presence of $-COOH$ (from PAA) after heating at 160 °C indicates that only partial cross-linking of the layers occurs, which is in agreement with earlier work.[19] Only about 10–15 % reduction in intensity of this peak was observed after heating the films. b) The amide bonds formed as a result of cross-linking (peak at $\nu \approx 1670$ $cm^{-1}$) are not discernible, largely because of the relatively low degree of cross-linking and masking from the peak at 1635 $cm^{-1}$ (arising from the APTS-BMS substrate and PAH).[19,22] c) The total amount of PAA deposited per APTS–BMS particle increases with PAA layer number, although the amount adsorbed per layer decreases with increasing PAA layer number (Figure 1 b).[25] This trend is attributed to increased blockage of the larger mesopores in the APTS–BMS templates with increasing PE layer number.

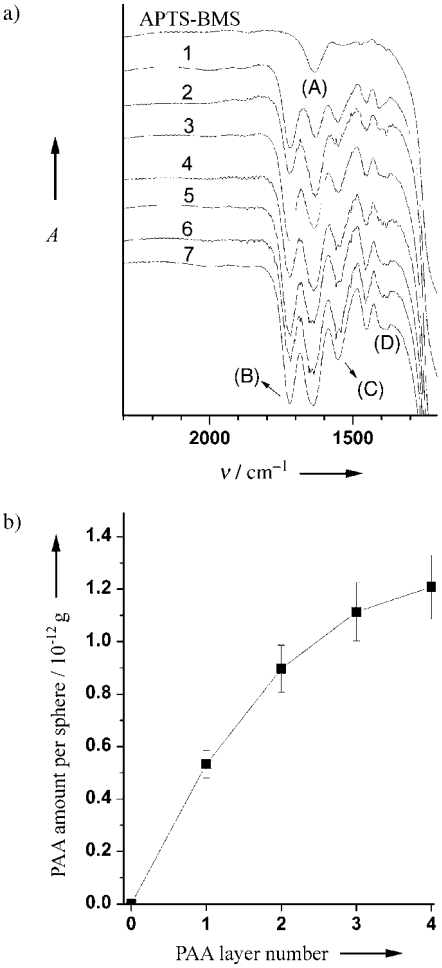


***Figure 1.*** a) FTIR spectra of the APTS–BMS spheres before and after the alternate deposition of PAA and PAH layers. The deposited layers were partially cross-linked by heating at 160 °C for 2 h prior to recording each spectrum. The numbers correspond to the number of PE layers deposited, commencing with PAA. APTS–BMS spheres were used as the internal reference for measuring each spectrum. The spectra are shifted vertically for clarity. b) The amount of PAA deposited on the APTS–BMS particle as a function of layer number was determined from the ratio of the peak at 1720 $cm^{-1}$ (PAA) with the peak at 800 $cm^{-1}$ (APTS–BMS).[25] The relative strength of the PAA signal compared to the APTS–BMS signal was determined to be 2.4 by measuring the IR spectrum of a 1:1 (weight) mixture of PAA and APTS–BMS powders. The APTS–BMS has an average weight of $4.3 \times 10^{-12}$ g, assuming the particle has a size of 2.5 μm and a density of 0.53 $g mL^{-1}$.

To examine the influence of sphere porosity, we used MS spheres with only 2–3 nm pores and nonporous silica spheres for comparison. No distinguishable peaks arising from PAA and PAH in the FTIR spectra of either of the PAA/PAH-coated silica spheres were observed, even after deposition of seven layers (i.e., 3.5 PAA/PAH bilayers). This result indicates that PE deposition predominantly occurs in the

  

larger mesopores of the APTS–BMS particles, and that the contribution to the FTIR intensities from PE adsorption on the outer surface of the particles is negligible.

Nitrogen adsorption measurements were also conducted to follow the changes in the surface area of the APTS–BMS spheres after PE deposition. The first layer of adsorbed PAA dramatically decreased the surface area from 465 $m^2 g^{-1}$ (APTS–BMS template) to 284 $m^2 g^{-1}$. This decrease is caused by the high PAA loading and blocking of some of the mesopores. Deposition of subsequent PAH and PAA layers resulted in a surface area decrease of approximately 20 $m^2 g^{-1}$per PE adsorption step. After deposition of seven layers, the surface area of the coated spheres was approximately 160 $m^2 g^{-1}$. These data further confirm the stepwise deposition of PEs within the APTS–BMS spheres.

NPS were prepared by exposing the PAA/PAH-coated APTS–BMS spheres to an aqueous 10 wt% HF solution for 12 h. Silica particles readily decompose in HF to form $[SiF_6]^{2-}$ ions, which can readily diffuse through PE multilayers.[26] Effective removal of the BMS template was demonstrated by energy-dispersive X-ray (EDX) analysis and FTIR experiments. EDX data showed that only a small amount of silicon (0.8%) was detected after removal of the BMS template (not shown). The small residual amount of silicon probably arises from silicon-alkyl groups ($\equiv$Si-$(CH_2)_3$-$NH_2$), which are stable in the presence of HF.[27] These groups are introduced into the sample through the APTS modification of the BMS particles.

Spherical NPS were obtained for samples that comprise two or more PAA and PAH layers. Figure 2 shows TEM and

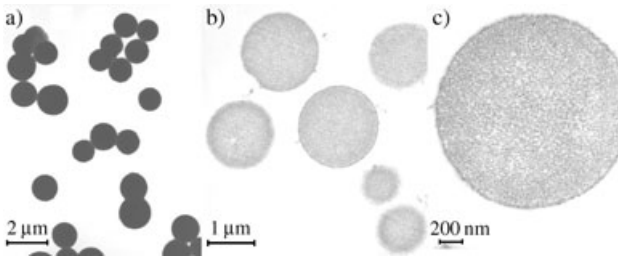


***Figure 2.*** TEM images of the NPS that comprises a) $(PAA/PAH)_2/PAA$ (5-NPS) and ultramicrotomed thin sections of the same spheres at b) low and c) higher magnification. The 5-NPS were partially cross-linked by heating at 160°C for 2 h after deposition of each PE layer. Images (b) and (c) show the porosity of the PE spheres. The large difference in the diameters seen is a result of the ultramicrotoming process.

Figure 3 SEM images of 5-layer $[(PAA/PAH)_2/PAA]$ NPS (5-NPS). These NPS retain the original shape of the BMS templates, and do not show signs of collapse, as is typically observed for PE capsules.[9] The diameters of the resulting NPS were found to depend on the number of PE layers deposited on the template APTS–BMS particles. APTS–BMS spheres coated with more PE layers underwent less shrinkage. For example, the PAA/PAH NPS (2-NPS) had diameters ranging from 0.8–1.3 μm, representing shrinkage of around 55–60%, compared with the original APTS–BMS templates, in which over 90% of APTS–BMS particles are within 2–3 μm. The 7-NPS were between 1.4–2.1 μm, 25–30% smaller than the template particles. No aggregation of the NPS was observed from TEM (Figure 2a). The inner structure of the NPS was examined by TEM of ultramicrotomed (approximately 90 nm thin slices) spheres. Figure 2b confirms that the PEs infiltrated into the BMS spheres, as PE can be seen in the interior of the NPS. At higher magnification (Figure 2c), a homogeneous porous structure with a pore size distribution of around 5–50 nm is clearly seen, confirming the nanoporosity of the spheres. SEM images of broken spheres (not shown) confirmed the interconnected PE network of the spherical particles. SEM also revealed the NPS to be individual particles, with no obvious aggregation of the particles observed (Figure 3a). At higher magnification, the roughness

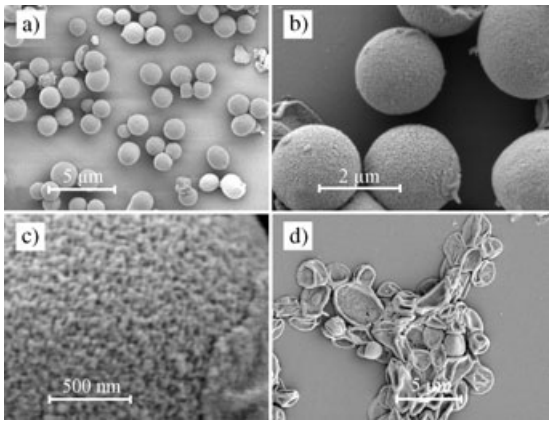


***Figure 3.*** SEM images of 5-NPS $[(PAA/PAH)_2/PAA]$ at different magnifications (a, b, c), and $(PAA/PAH)_2/PAA$ capsules prepared when PAA and PAH are deposited in the absence of added salt in the adsorption solution (d). The 5-NPS and capsules were partially cross-linked by heating at 160°C for 2 h after deposition of each PE layer.

and porosity of the spheres is apparent (Figure 3b), with homogeneous pores in the range of approximately 10–50 nm seen (Figure 3c). Figure 3d shows the collapsed capsule structure of the product prepared by the same procedure when the PE layers were deposited in the absence of salt. This indicates that, as mentioned above, the salt facilitates PE coiling and penetration into the mesopores of the BMS templates. In the absence of salt, the PEs assume a more linear conformation[18] and therefore will be mainly restricted to the surface. We note that the highly efficient role of the APTS–BMS spheres as templates for the preparation of interconnected porous particles is attributed to the abundant and disordered pore structure of the larger mesopores and high surface area (465 $m^2 g^{-1}$) of the APTS–BMS particles. For example, a recent study employing porous (radial channel-like) $CaCO_3$ microparticle templates (surface area ca. 8.8 $m^2 g^{-1}$) resulted in PE microcapsules that collapse when dried,[15] which is in stark contrast to the free-standing NPS reported herein.

The capacity of the NPS as hosts for the immobilization of biomacromolecules was investigated through lysozyme adsorption studies. Approximately 10 mg of the NPS were dispersed in 15 mL of a 1 mg $mL^{-1}$ lysozyme ($M_w = 14.6$ kDa) solution containing 50 mM phosphate buffer (pH 7.0). The

  

immobilization and distribution of enzyme in the NPS were examined by confocal laser scanning microscopy (CLSM). Figure 4 shows the CLSM images of the 5-NPS after incubation in fluorescein isothiocyanate-labeled lysozyme

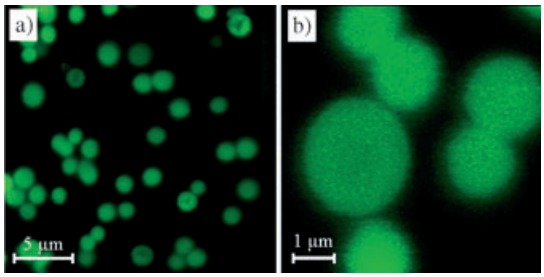


***Figure 4.*** CLSM images of FITC-labeled lysozyme immobilized in the 5-NPS at a) low and b) higher magnification. The 5-NPS were partially cross-linked by heating at 160 °C for 2 h after deposition of each PE layer.

(FITC-lysozyme) for 1 h, and subsequent washing with water. The images show that FITC-lysozyme is distributed homogeneously throughout the NPS. The amount of enzyme immobilized by the NPS was determined spectrophotometrically by measuring the difference in lysozyme absorbance at 280 nm before and after adsorption. For the 5-NPS, the weight of the NPS increased by approximately 90 % after lysozyme immobilization, corresponding to $6.7 \times 10^{-17}$ mol of lysozyme per sphere. This value corresponds to a concentration of about 470 mg mL$^{-1}$ of lysozyme in 5-NPS, which is approximately a factor of two times larger than that obtained for the direct immobilization of lysozyme onto BMS spheres under the same conditions (220 mg mL$^{-1}$), and for that reported for bovine serum albumin in poly(styrene sulfonate)/PAH capsules with a "matrix-type interior" (250 mg mL$^{-1}$).[15] The high enzyme immobilization capacity of the NPS is attributed to the nanoporous PE framework in the NPS.

In conclusion, intact NPS with an interconnected PE network have been prepared by the LbL assembly of PEs onto APTS–BMS spheres and subsequent removal of the template. Electron microscopy data show that the NPS have pores ranging from 5–50 nm. The NPS show excellent capacity for immobilization of enzymes (lysozyme). Since the LbL method is amenable to the deposition of diverse PEs, the preparation of NPS of controlled composition and functionality can be achieved by the reported approach. This feature will facilitate designing NPS for the uptake of various species, such as macromolecules, low-molecular-weight drugs, pesticides and fragrances, and nanoparticles through, for example, electrostatic association or hydrogen bonding with the NPS host. The broad range of MS materials available with tunable size, morphology and porosity will enable the preparation of tailored porous PE materials that are envisaged to find application in biocatalysis, separation technology, and controlled drug delivery systems.

Received: September 28, 2004
Revised: December 1, 2004
Published online: April 7, 2005

**Keywords:** layer-by-layer technique · mesoporous materials · nanoporous spheres · polyelectrolytes · silica

[1] T. Yanagisawa, T. Shimizu, K. Kuroda, C. Kato, *Bull. Chem. Soc. Jpn.* **1990**, *63*, 988.
[2] T. Kresge, M. E. Leonowicz, W. J. Roth, J. C. Vartuli, J. S. Beck, *Nature* **1992**, *359*, 710.
[3] a) Z. Liu, Y. Sakamoto, T. Ohsuna, K. Hiraga, O. Terasaki, C. H. Ko, H. J. Shin, R. Ryoo, *Angew. Chem.* **2000**, *112*, 3237; *Angew. Chem. Int. Ed.* **2000**, *39*, 3107; b) Y. J. Han, J. M. Kim, G. D. Stucky, *Chem. Mater.* **2000**, *12*, 2068; c) K.-B. Lee, S.-M. Lee, J. Cheon, *Adv. Mater.* **2001**, *13*, 517; d) T. A. Crowley, K. J. Ziegler, D. M. Lyons, D. Erts, H. Olin, M. A. Morris, J. D. Holmes, *Chem. Mater.* **2003**, *15*, 3518.
[4] a) B. Tian, X. Liu, H. Yang, S. Xie, C. Yu, B. Tu, D. Zhao, *Adv. Mater.* **2003**, *15*, 1370; b) K. Zhu, B. Yue, W. Zhou, H. He, *Chem. Commun.* **2003**, 98; c) A. Dong, N. Ren, Y. Tang, Y. Wang, Y. Zhang, W. Hua, Z. Gao, *J. Am. Chem. Soc.* **2003**, *125*, 4976.
[5] a) R. Ryoo, S. H. Joo, S. Jun, *J. Phys. Chem. B* **1999**, *103*, 7743; b) R. Ryoo, S. H. Joo, M. Kruk, M. Jaroniec, *Adv. Mater.* **2001**, *13*, 677; c) C. Yu, J. Fan, B. Tian, D. Zhao, G. D. Stucky, *Adv. Mater.* **2002**, *14*, 1742.
[6] a) C. G. Goltner, S. Henke, M. C. Weissenberger, M. Antonietti, *Angew. Chem.* **1998**, *110*, 633; *Angew. Chem. Int. Ed. Engl.* **1998**, *37*, 613; b) K. Kageyama, J.-I. Tamazawa, A. Aida, *Science* **1999**, *285*, 2113; c) J. Y. Kim, S. B. Yoon, F. Kooli, J. Yu, *J. Mater. Chem.* **2001**, *11*, 2912; d) E. Yilmaz, O. Ramsrtöm, P. Möller, D. Sanchez, K. Mosbach, *J. Mater. Chem.* **2002**, *12*, 1577.
[7] a) U. Meyer, A. Larsson, H. P. Hentze, R. A. Caruso, *Adv. Mater.* **2002**, *14*, 1768; b) D. G. Shchukin, R. A. Caruso, *Chem. Commun.* **2003**, 1478; c) O. Norrlöw, M. Glad, K. Mosbach, *J. Chromatogr.* **1984**, *299*, 29; d) A. G. Mayes, K. Mosbach, *Anal. Chem.* **1996**, *68*, 3769.
[8] a) G. Decher, J. D. Hong, *Ber. Bunsen-Ges.* **1991**, *95*, 1430; b) G. Decher, *Science* **1997**, *277*, 1232.
[9] For reviews, see: a) F. Caruso, *Adv. Mater.* **2001**, *13*, 11; b) F. Caruso, *Chem. Eur. J.* **2000**, *6*, 413; c) C. S. Peyratout, L. Dähne, *Angew. Chem.* **2004**, *116*, 3850; *Angew. Chem. Int. Ed.* **2004**, *43*, 3762.
[10] a) C. Tedeschi, F. Caruso, H. Möhwald, S. Kirstein, *J. Am. Chem. Soc.* **2000**, *122*, 5841; b) A. A. Mamedov, A. Belov, M. Giersig, N. N. Mamedova, N. A. Kotov, *J. Am. Chem. Soc.* **2001**, *123*, 7738; c) W. Jin, X. Shi, F. Caruso, *J. Am. Chem. Soc.* **2001**, *123*, 8121.
[11] a) F. Caruso, R. A. Caruso, H. Möhwald, *Science* **1998**, *282*, 1111; b) E. Donath, G. B. Sukhorukov, F. Caruso, S. A. Davis, H. Möhwald, *Angew. Chem.* **1998**, *110*, 2323; *Angew. Chem. Int. Ed. Engl.* **1998**, *37*, 2201; c) F. Caruso, H. Lichtenfeld, E. Donath, H. Möhwald, *Macromolecules* **1999**, *32*, 2317.
[12] D. Wang, F. Caruso, *Chem. Commun.* **2001**, 489.
[13] Z. Liang, A. S. Susha, A. Yu, F. Caruso, *Adv. Mater.* **2003**, *15*, 1849.
[14] a) S. Ai, G. Lu, Q. He, J. Li, *J. Am. Chem. Soc.* **2003**, *125*, 11140; b) S. Hou, C. Harrell, L. Trofin, P. Kohli, C. R. Martin, *J. Am. Chem. Soc.* **2004**, *126*, 5674.
[15] a) D. V. Volodkin, A. I. Petrov, M. Prevot, G. B. Sukhorukov, *Langmuir* **2004**, *20*, 3398; b) G. B. Sukhorukov, D. V. Volodkin, A. M. Günther, A. I. Petrov, D. B. Shenoy, H. Möhwald, *J. Mater. Chem.* **2004**, *14*, 2073.
[16] G. Schulz-Ekloff, J. Rathouský, A. Zukal, *Int. J. Inorg. Mater.* **1999**, *1*, 97.
[17] In this process, the dried BMS powder was dispersed in toluene by sonication for 20 min before APTS was added to the suspension. The molar ratio of the BMS particles (calculated as $SiO_2$:APTS:toluene) was fixed at 5:1:500, and the suspension was heated under reflux for 24 h. The APTS-grafted BMS

  

particles were separated from the solution by centrifugation, and washed in toluene and methanol twice, respectively. Finally, the pellet was dried at 80 °C for 12 h.
[18] G. Decher, J. Schmitt, *Prog. Colloid Polym. Sci.* **1992**, *89*, 160.
[19] J. J. Harris, P. M. DeRose, M. L. Bruening, *J. Am. Chem. Soc.* **1999**, *121*, 1978.
[20] P. Schuetz, F. Caruso, *Adv. Funct. Mater.* **2002**, *13*, 929.
[21] Under the conditions used (low $M_w$ PEs and relatively high NaCl concentrations), partial desorption of the adsorbed PE layer by the incoming PE from solution occurs. Such effects ("PE stripping") have been been observed before (Z. Sui, D. Salloum, J. B. Schlenoff, *Langmuir* **2003**, *19*, 2491). Sonication may also cause some removal of adsorbed PE.
[22] R. Takahashi, S. Sato, T. Sodesawa, M. Kawakita, K. Ogura, *J. Phys. Chem. B* **2000**, *104*, 12184.
[23] J. L. Stair, J. J. Harris, M. L. Bruening, *Chem. Mater.* **2001**, *13*, 2641.
[24] D. Yoo, S. S. Shiratori, M. F. Rubner, *Macromolecules* **1998**, *31*, 4309.
[25] Since the peak around 1635 $cm^{-1}$ is a combination of the Si–OH vibration of the APTS–BMS spheres and the N–H bending (scissoring) vibrations of the APTS and PAH, and overlaps with the amide band owing to film cross-linking, calculation of the adsorbed amount of PAH is complicated. Therefore, we chose to analyze the peak at 1720 $cm^{-1}$ originating from PAA.
[26] L. Dähne, B. Baude, A. Voigt, Patent WO 2004/014540A1, **2003**.
[27] a) J. Choi, J. Harcup, A. F. Yee, Q. Zhu, R. M. Laine, *J. Am. Chem. Soc.* **2001**, *123*, 11420; b) R. O. R. Costa, W. L. Vasconcelos, *Macromolecules* **2001**, *34*, 5398.

  